Supporting Information

Ruthenium nanoparticles supported on Ni_3N nanosheets as bifunctional electrocatalysts for hydrogen oxidation/evolution reactions

Ziheng Liang, Huibing Liu, Shiqing Huang, Minghui Xing, Zhenyang Li, Shitao Wang, Liu Yang*, Dapeng Cao*

State Key Laboratory of Organic-Inorganic Composites, Beijing University of Chemical Technology, Beijing 100029, P. R. China

* E-mail: yl@mail.buct.edu.cn, caodp@mail.buct.edu.cn

Material synthesis

Synthesis of Ru/Ni_3N-NF:

In a typical synthesis of Ru/Ni_3N-NF, firstly, several Ni foams (NF) were cut into 2*4cm and then washed by hydrochloric acid and deionized water. Then, 1.8mmol $Ni(NO)_3 \cdot 6H_2O$, 4mmol NH_4F and 7.5mmol urea were added into the solution. After stirring for 15 minutes and everything was dissolved, the solution was transferred into a 50mL Teflon-lined autoclave. After that, put the NF into the autoclave leaning against it and the autoclave was heated at 120℃ for 6h. After the autoclave was

cooled to room temperature, then the $Ni(OH)_2$-NF was prepared and washed by H_2O for several times. Then, 10 mmol $RuCl_3 \cdot 2H_2O$ was dissolved in 25mL deionized water and the solution was transferred into an electrolyzer. Then we used a standard three-electrode system to finish the electrodeposition process. The Ru/$Ni(OH)_2$-NF was cut into 1.5*2cm and put on the working electrode, while the carbon rod was put on the counter electrode and the calomel electrode was used as a reference electrode. We used the i-t curve technique and for the parameters, the initial voltage was -1V and the time was 3600s and the Ru/$Ni(OH)_2$-NF was prepared. At last, the Ru/$Ni(OH)_2$-NF was put into a pipe furnance. The furnace was purged with ammonia for 30 minutes first, and then the material was heated at 400℃ for 3 h with a ramp rate of 10℃/min and the Ru/Ni_3N-NF was successfully prepared.

Synthesis of Ni_3N-NF:

In a typical synthesis of Ni_3N-NF, the process was the same as that of Ru/Ni_3N-NF without the electrodeposition process of Ru.

Synthesis of Ru-NF:

In a typical synthesis of Ru-NF, the process was the same as that of Ru/Ni_3N-NF except the precursor was NF instead of $Ni(OH)_2$-NF.

Physical characterization:

The X-ray powder diffraction (XRD) patterns were recorded on a Japan Rigaku Smart Lab TM rotation anode X-ray diffractometer with Cu Kα radiation (λ = 0.154 nm). The scanning electron microscope (**SEM**) images of the samples were obtained from S-4800. High-resolution TEM (**HRTEM**) and energy-dispersive X-ray

spectrometry (**EDX**) elemental mapping were performed using an FEI Tecnai G2 F30 Super-Twin high-resolution transmission electron microscope at an accelerating voltage of 300 kV. The X-ray photoelectron spectroscopy (**XPS)** was performed on a Thermo Scientific 250 X-ray photoelectron spectrometer using Al Ka radiation. Inductively coupled plasma (**ICP**) data were obtained by using an Agilent ICP-OES 725 ES instrument. Extended X-ray Absorption Fine Structure **(EXAFS)** was performed at the Singapore Synchrotron Light Source (SSLS) center, where a pair of Chanel-cut Si (111) crystals was used in the monochromator. The Ru K-edge XANES data were recorded in a transmission mode. Ru powder was used as reference. The storage ring was working at the energy of 2.5 GeV with an average electron current of below 200 mA. The acquired EXAFS data were extracted and processed according to the standard procedures using the ATHENA module implemented in the FEFIT software packages. The k^2-weighted Fourier transform (FT) of x(k) in R space was obtained over a range of 0-14.0 $Å^{-1}$ by applying a Besse window function.

Electrochemical measurements:

A standard three-electrode system was applied for the electrochemical measurements. The as-synthesized Ru/Ni_3N-NF, Ni_3N-NF, Ru-NF and Pt/C catalysts were directly used as working electrodes. We used a saturated calomel electrode (SCE) and a graphite rod as the reference electrode and counter electrode, respectively. The results were converted to the RHE reference scale using the following equation:

$$E\ (vs\ RHE) = E\ (vs\ SCE) + 0.2415 + 0.059 \times pH$$

The commercial Pt/C was loaded on a pure nickel foam (1×1 cm) with the optimal loading we measured (1 mg/cm^{-2}). When testing the HOR performance, to ensure the solution was saturated, the electrolyte was bubbled with Ar gas for 20 min and then with H_2 gas for at least 30 min. All the data of linear sweep voltammetry (LSV), cyclic voltammetry (CV) curves without instrument were iR-corrected.

The exchange current density (i_0) was acquired by the micro-polarization region (from -3 to 3 mV). And the Butler-Volmer can be simplified through expanded by Talyor's formula as below:

$$i = i_0 \eta F/RT$$

where i is the overall current density, η is the overpotential, R is the ideal gas constant (8.314 J mol^{-1} K^{-1}), F is the Faraday's constant (96485 C mol^{-1}) and T is the experimental temperature (298K).

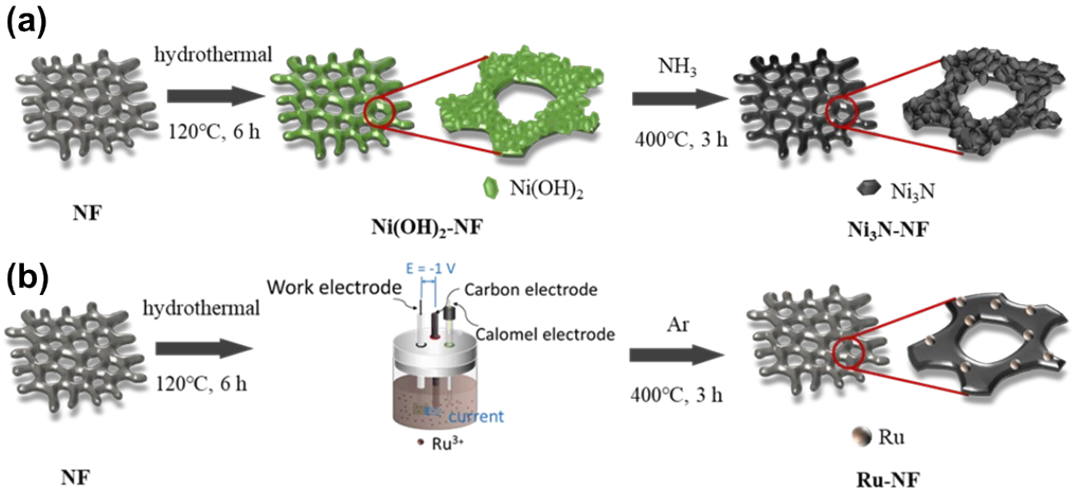

Figure S1. The preparation process of (a) Ni_3N-NF and (b) Ru-NF

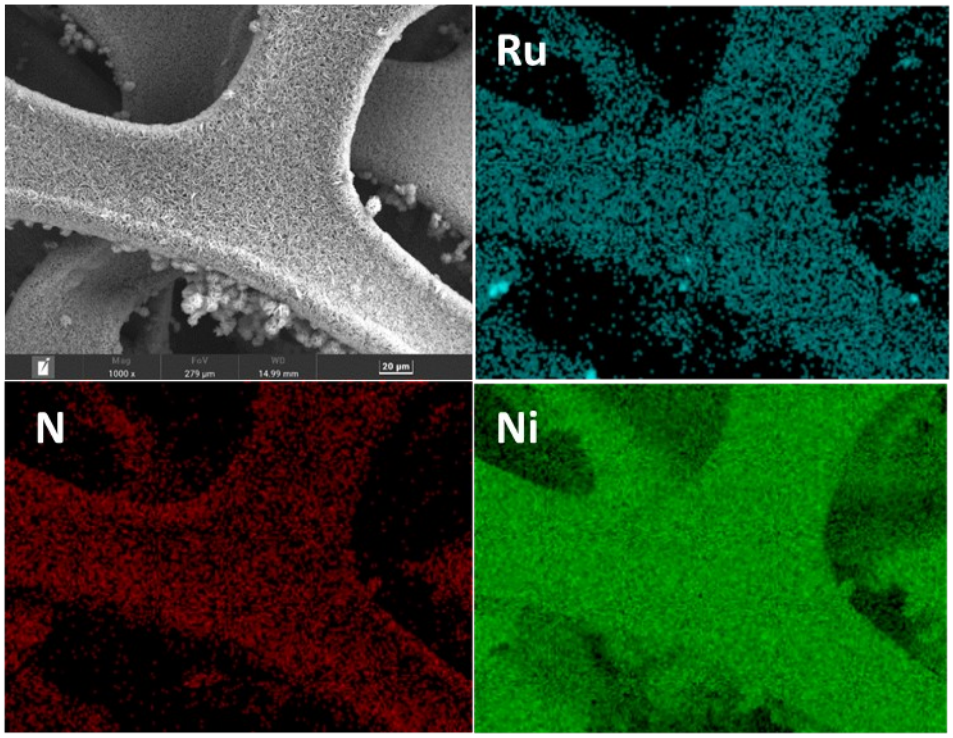

Figure S2. Elemental mapping images of SEM for Ru/Ni_3N-NF.

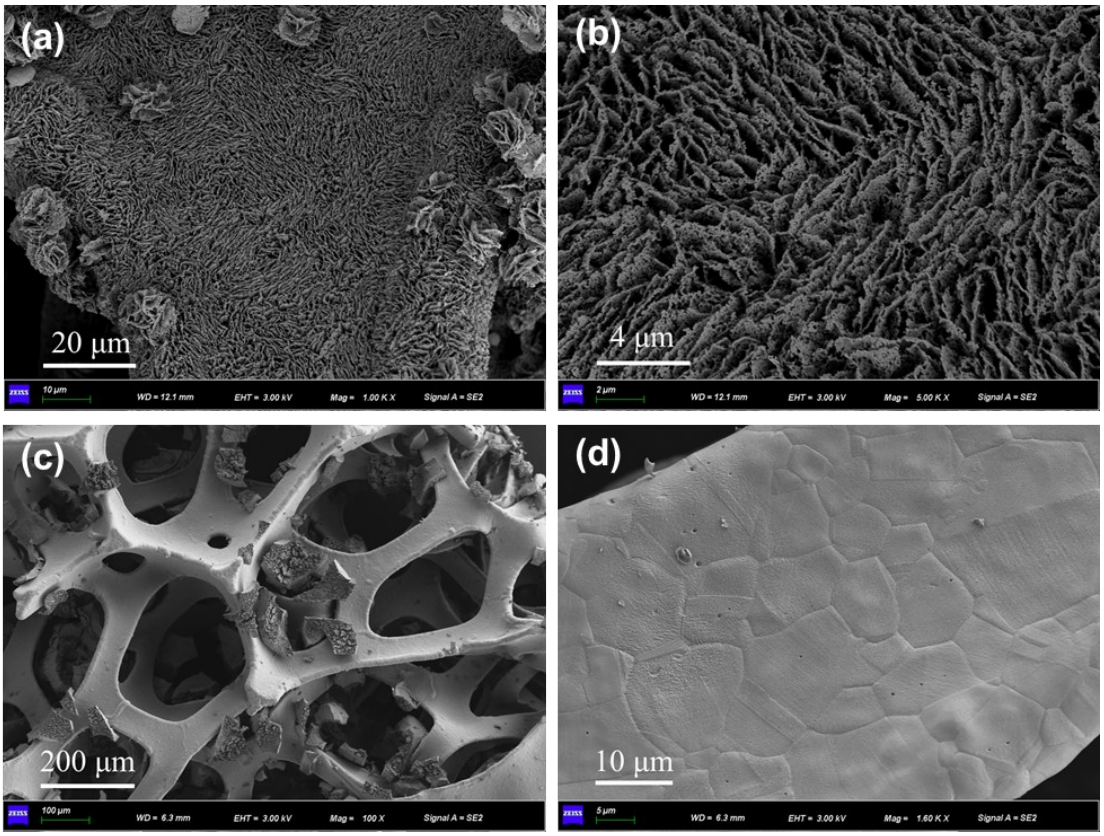

Figure S3. The SEM images of (a, b) Ni_3N-NF and (c, d) Ru-NF.

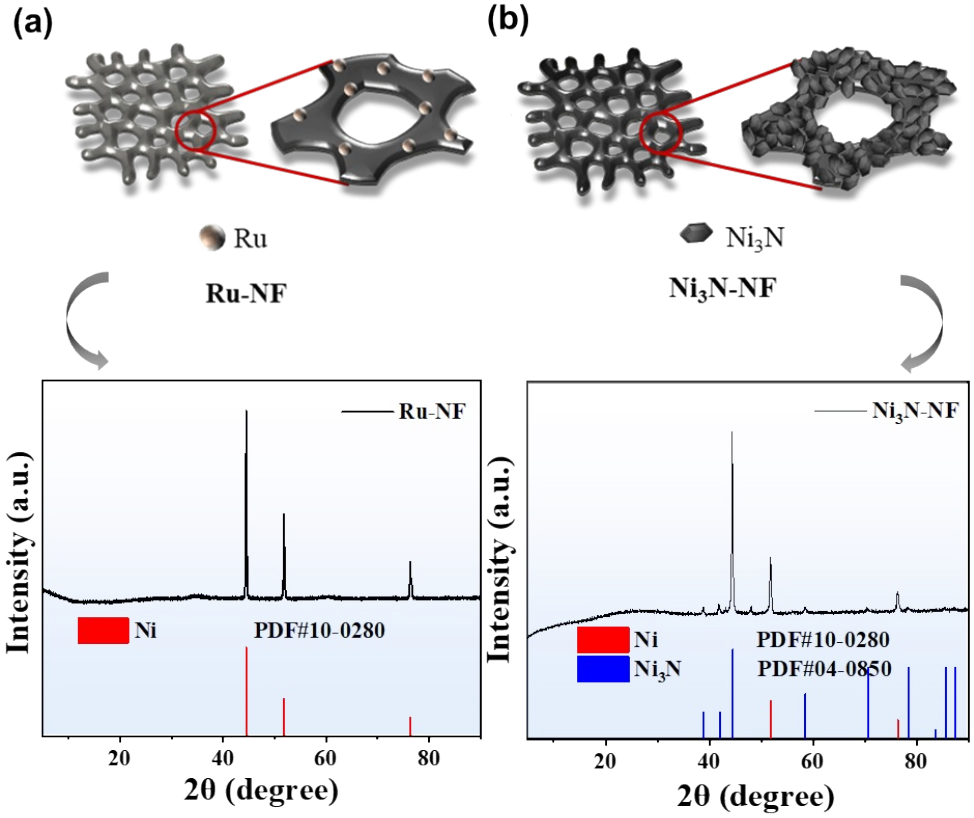

Figure S4. The schematic diagram and corresponding XRD spectra of (a) Ru-NF and (b) Ni_3N-NF.

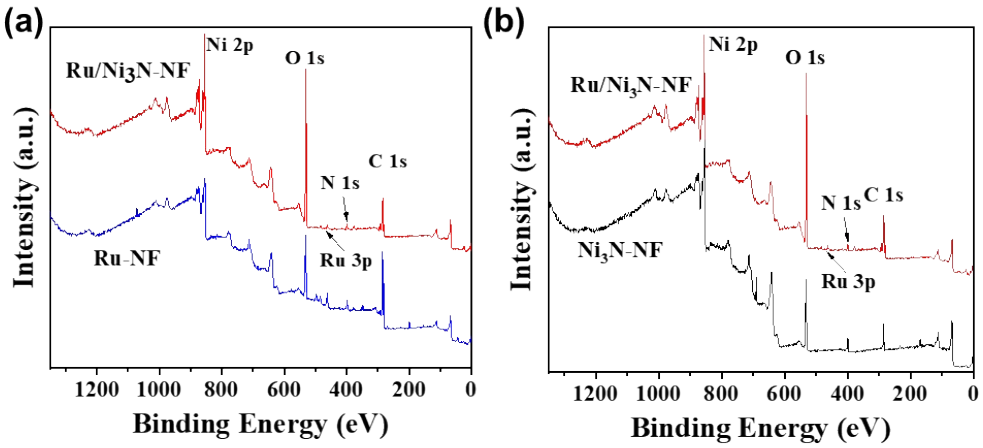

Figure S5. The XPS survey scan of Ru/Ni_3N-NF, Ru-NF and Ni_3N-NF.

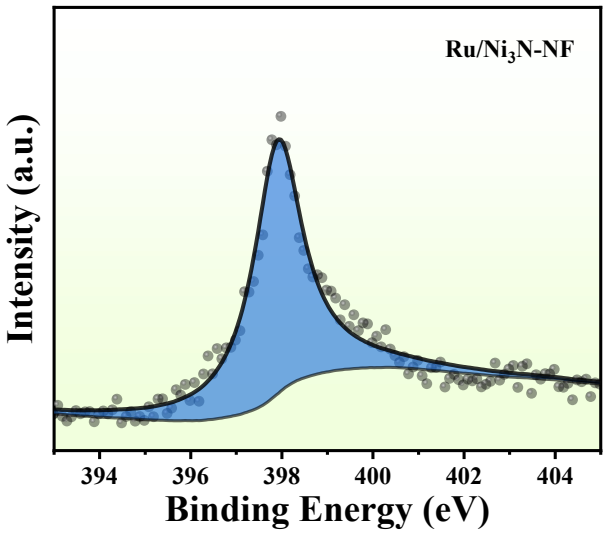

Figure S6. The N 1s XPS spectra of Ru/Ni_3N-NF.

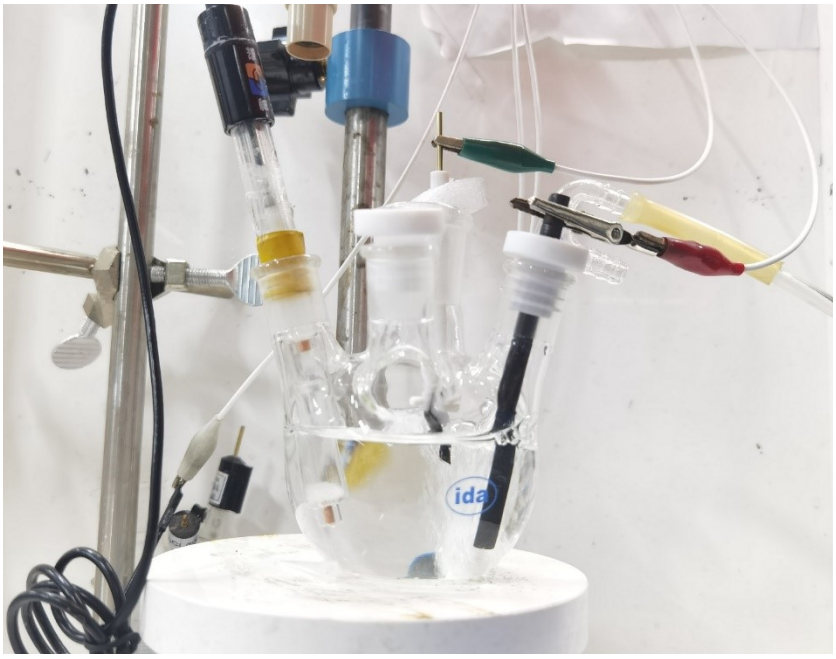

Figure S7. The three-electrode system used to the measurement of HOR performances. The solution is 0.1 M KOH, and the bubbles are injected H_2.

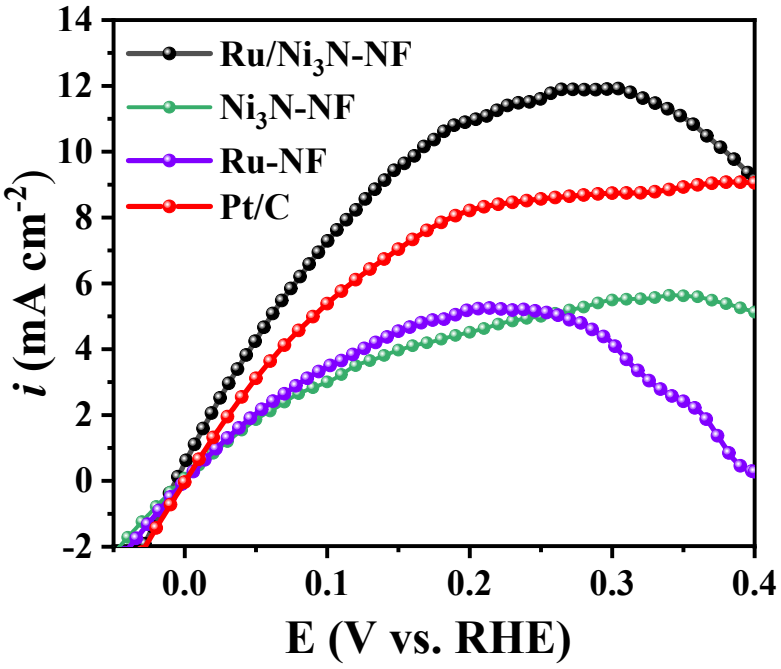

Figure S8. HOR polarization curves in H_2 saturated 0.1 M KOH with a scan rate of 1 mV s^{-1} without iR-corrected.

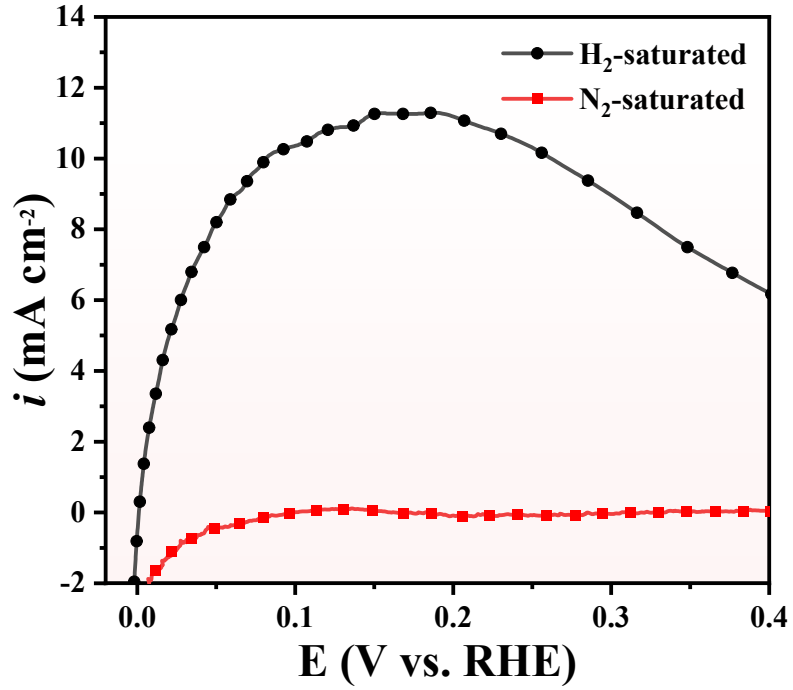

Figure S9. HOR polarization curves Ru/Ni_3N-NF in H_2-saturated and N_2-saturated 0.1M KOH solution with a scan rate of 1 mV s^{-1}.

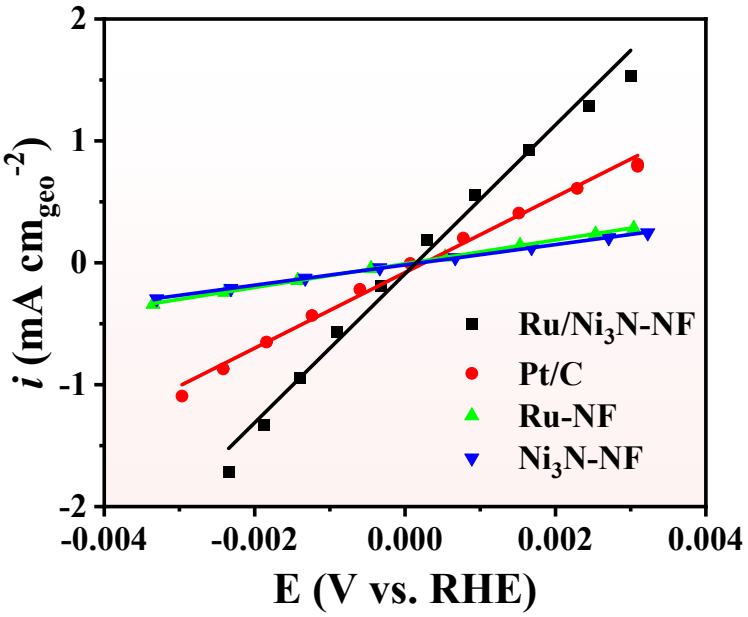

Figure S10. Micro-polarization region (-3 mV to 3 mV) of Ru/Ni_3N-NF, Ru-NF, Ni_3N-NF and Pt/C, respectively. The lines indicate the linear fitting.

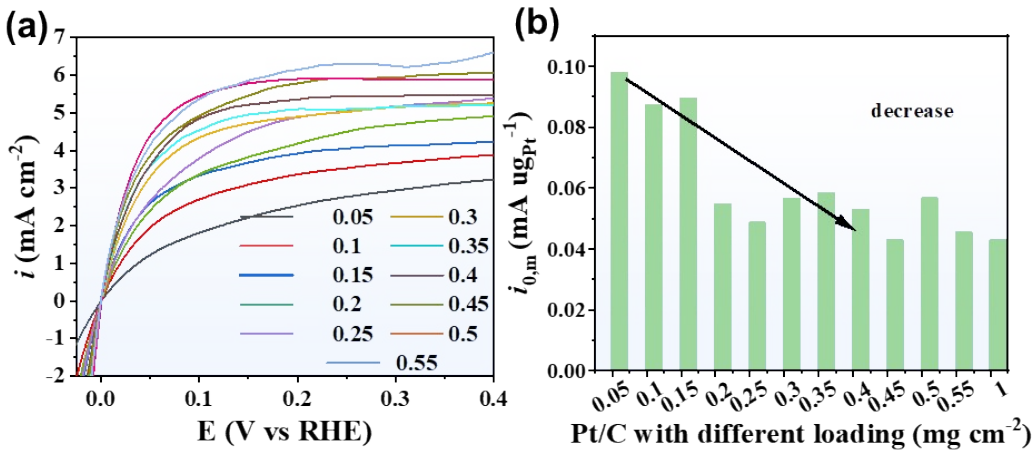

Figure S11. The (a) LSV curves and (b) $i_{0,m}$ of Pt/C with different loading of 0.05 ~ 0.55 mg cm^{-2}.

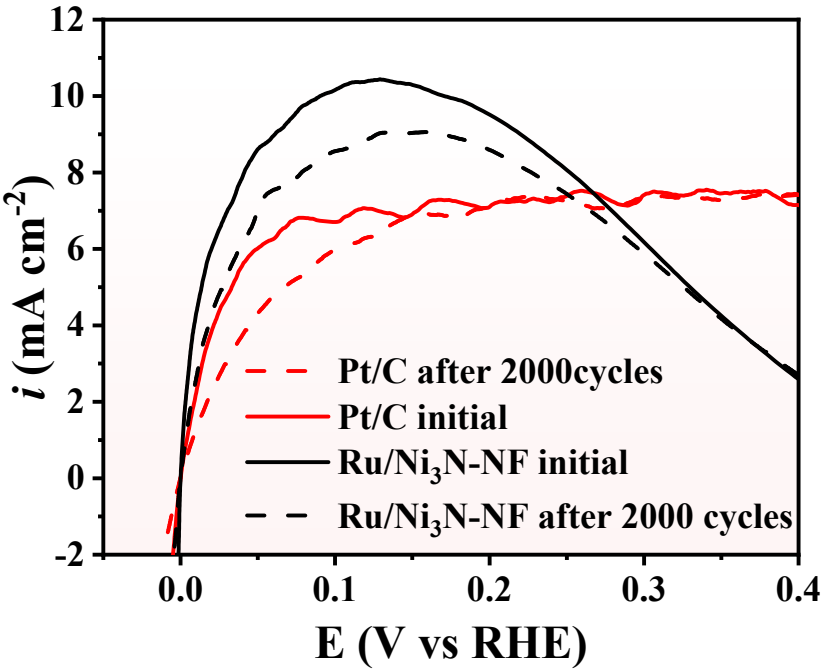

Figure S12. The HOR polarization curves for Ru/Ni_3N-NF and Pt/C before and after ADT.

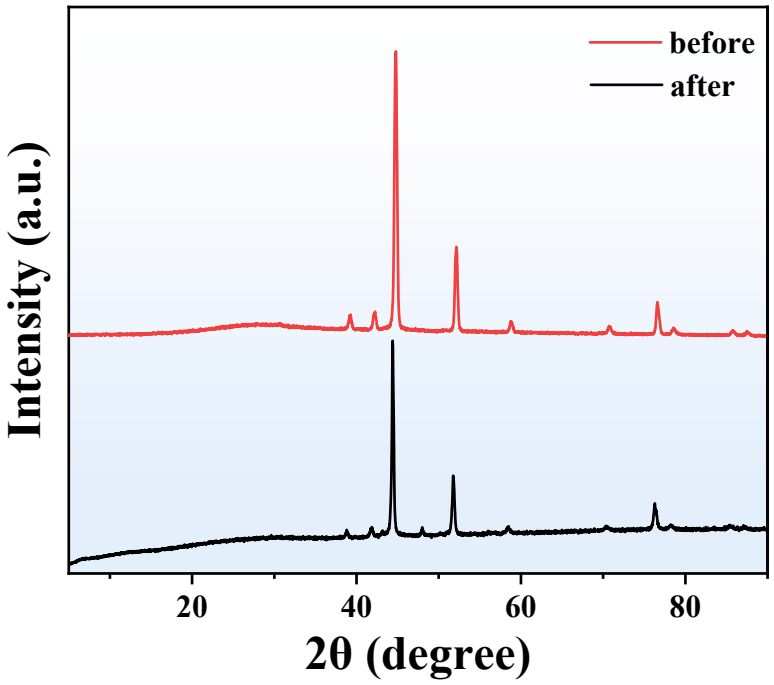

Figure S13. The XRD spectrum of Ru/Ni_3N-NF before and after the stability test.

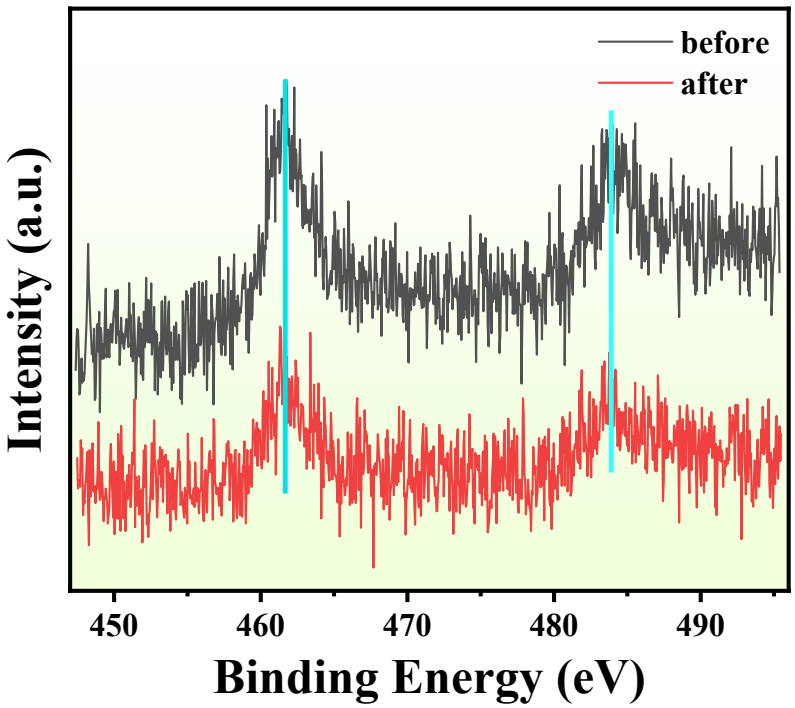

Figure S14. The Ru 3p spectrum of Ru/Ni_3N-NF before and after the stability test.

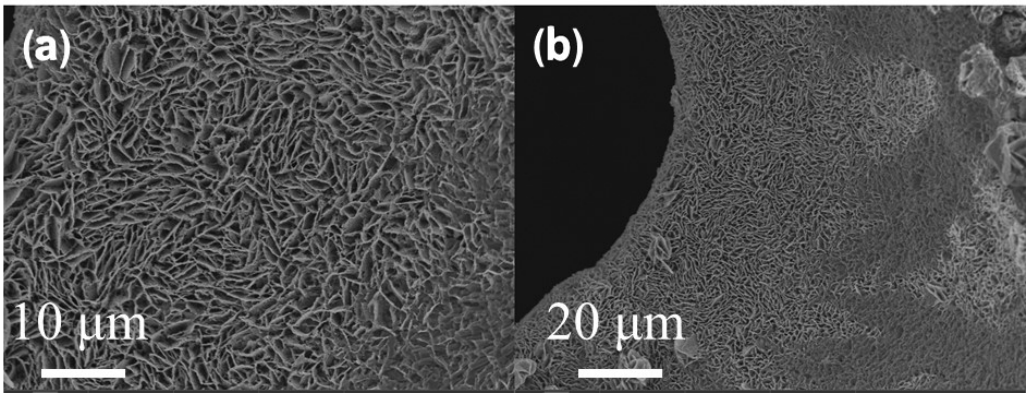

Figure S15. The SEM spectrums of Ru/Ni_3N-NF after the stability test.

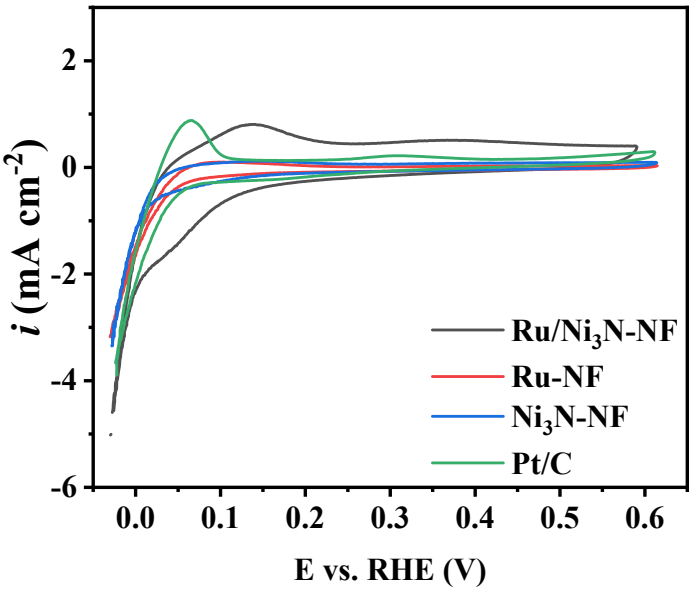

Figure S16. Cyclic voltammograms of Ru/Ni_3N-NF, Ru-NF, Ni_3N-NF and Pt/C in Ar-saturated 0.1 M KOH at a scan rate of 1 mV s^{-1}.

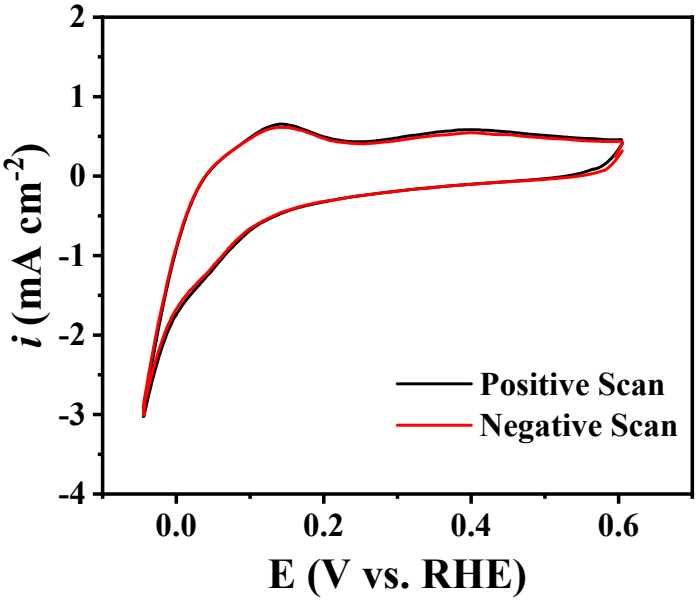

Figure S17. Cyclic voltammograms of Ru/Ni_3N-NF in Ar-saturated 0.1 M KOH at a scan rate of 1 mV s^{-1}.

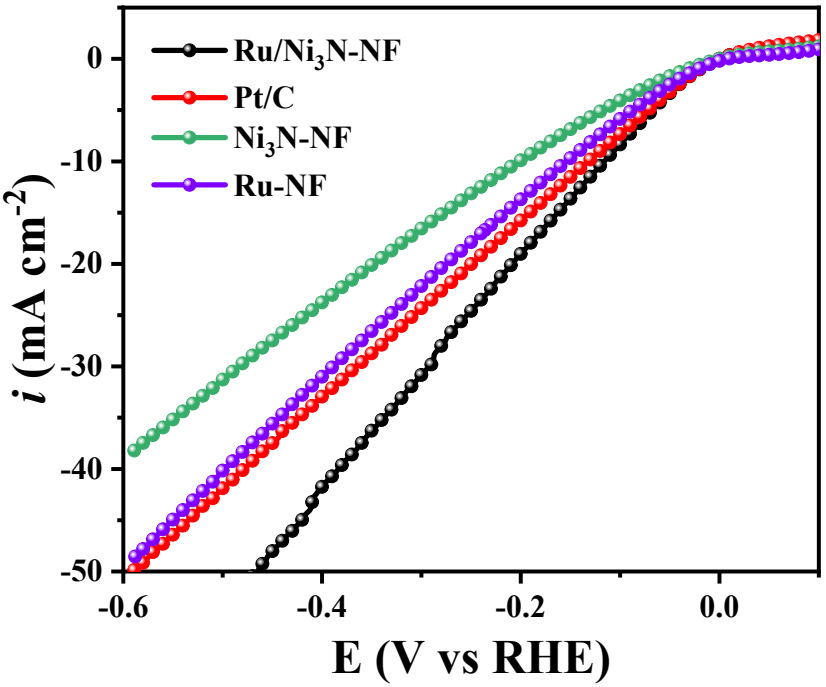

Figure S18. HER polarization curves without iR-corrected in 0.1 M KOH with a scan rate of 5 mV s^{-1}.

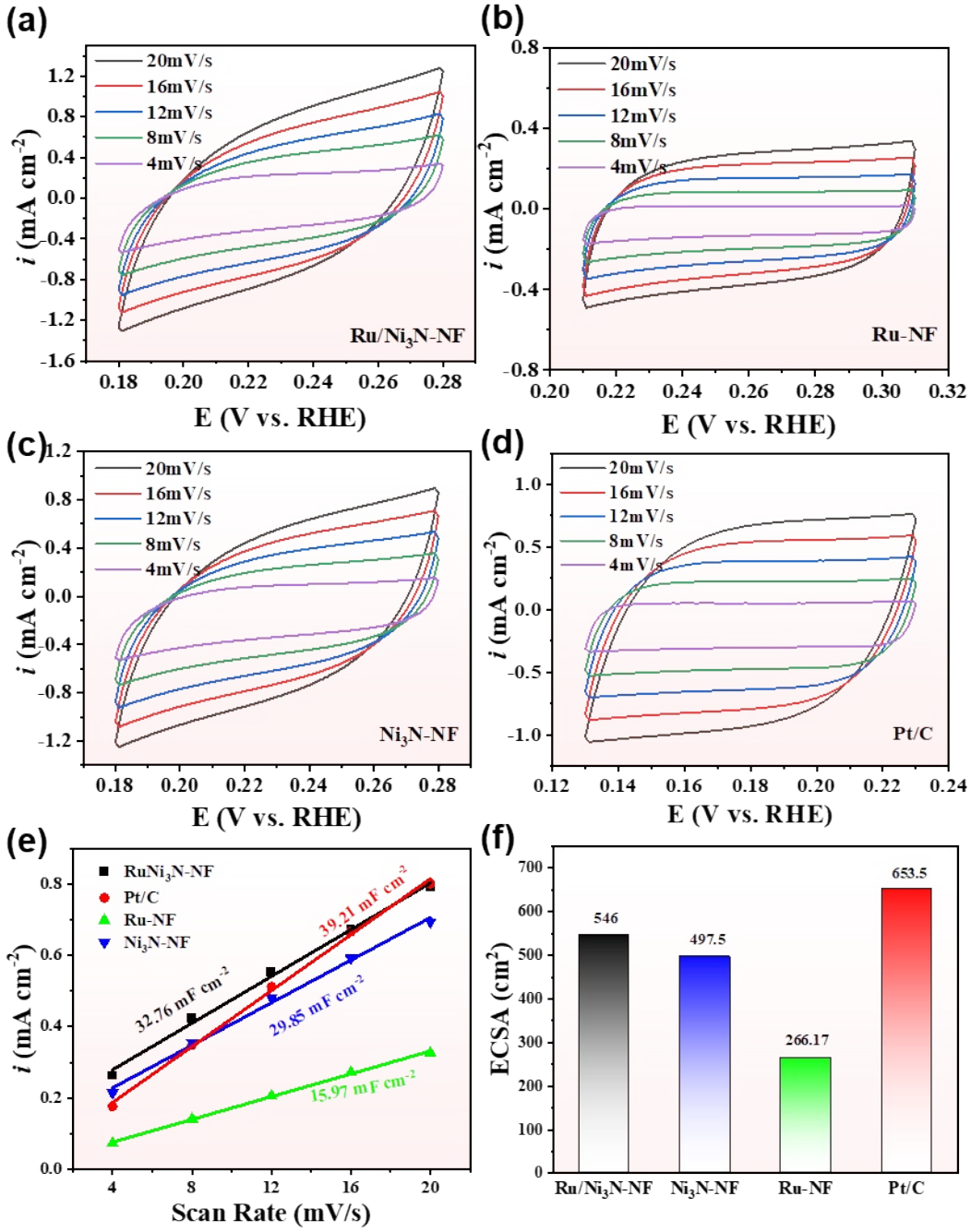

Figure S19. CV measurements for (a) Ru/ Ni_3N-NF, (b) Ru-NF, (c) Ni_3N-NF and (d) Pt/C in the 0.1 M KOH solution; (e) The linear fitting of scan rate versus $\triangle i$ (the difference between the anodic and cathodic current densities at open circuit potential); (f) The ECSA of prepared catalysts. The resulting linear slope the C_{dl} and the ECSA can be calculated according to the following equation: ECSA = C_{dl}/C_s, where Cs is the specific capacitance which is generally found to be in the range of 20~60 μF cm^{-2}. Here, 60 μF cm^{-2} was used in the following calculations of the ECSA as literatures generally did.

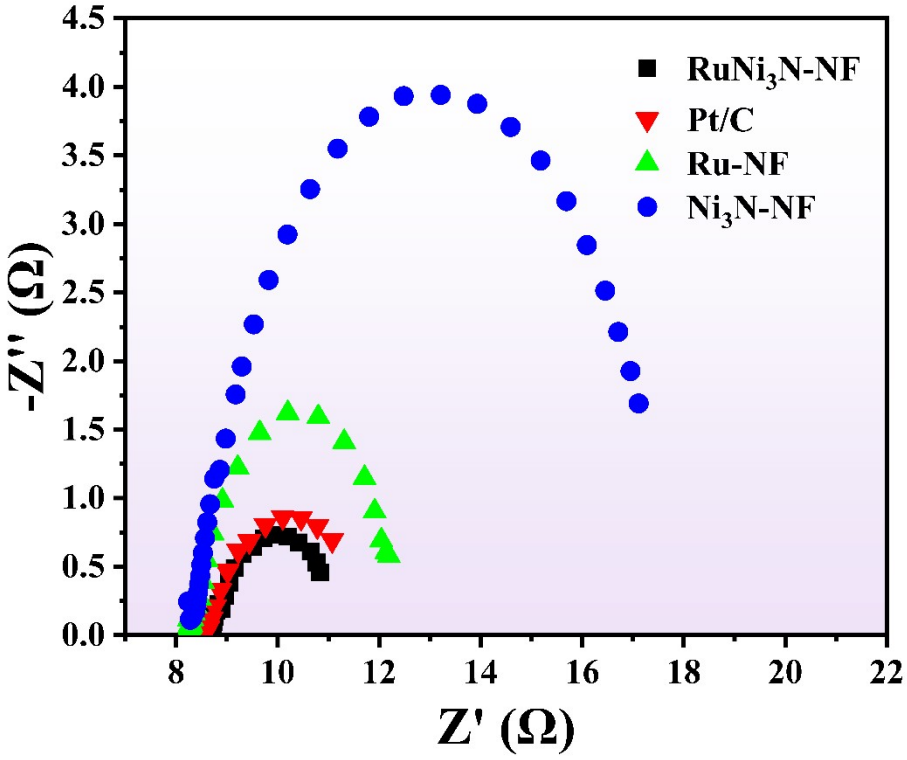

Figure S20. The Nyquist plots of Ru/ Ni_3N-NF, Ni_3N-NF, Ru-NF and Pt/C. The EIS are conducted in 0.1M KOH under a 50 mV overpotential.

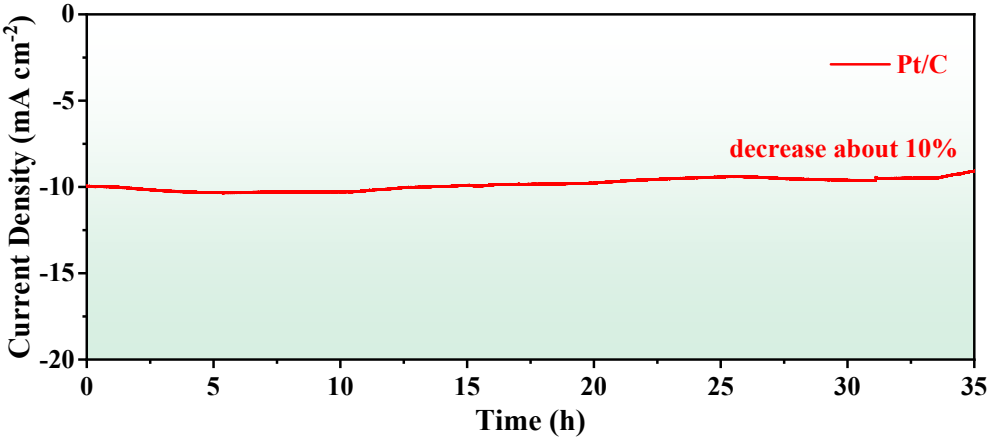

Figure S21. Chronoamperometry test of Pt/C at an initial current density of 10 mA cm^{-2}

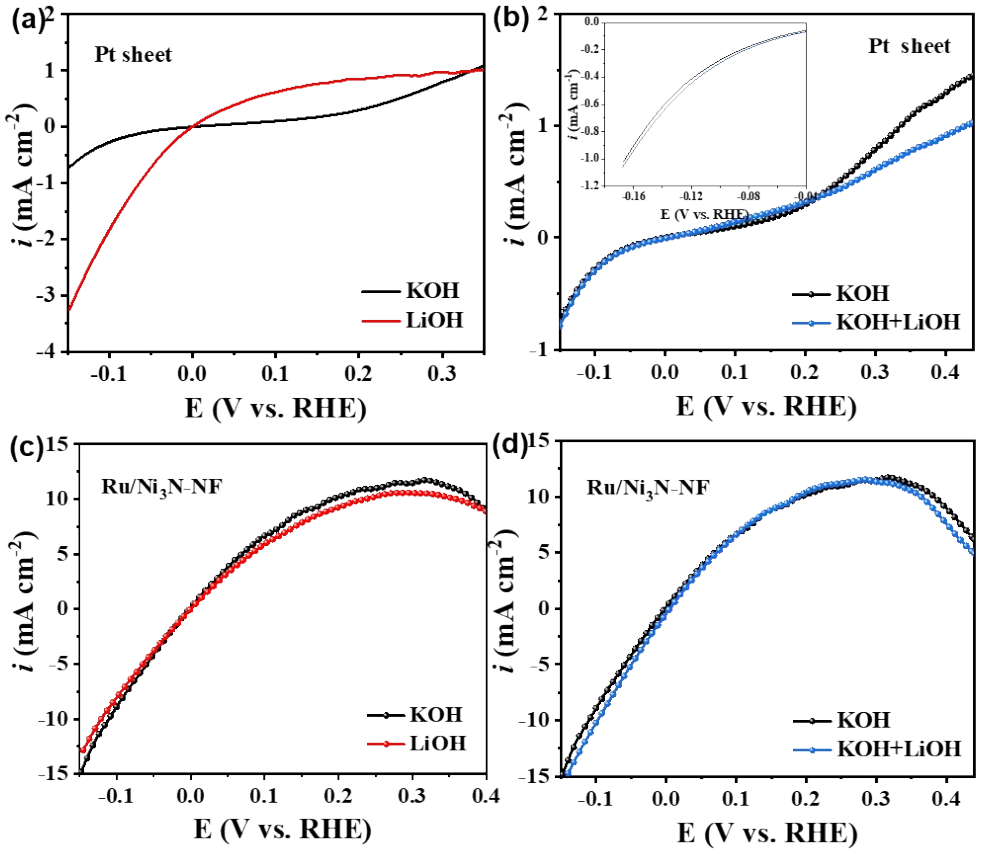

Figure S22. HOR polarization curves of (a, b) Pt bulk and (c, d) Ru/Ni_3N-NF in H_2-saturated 0.1 M KOH, 0.1 M KOH + 5 mM LiOH and 0.1 M LiOH with a scan rate of 1 mV s^{-1}

Table S1. ICP-OES analysis Ru/Ni_3N-NF

Catalyst	Mass of catalyst (mg)	wt % Ru	Mass density (ug cm^{-2})
Ru/Ni_3N-NF-1	25.2	0.0782	19.71
Ru/Ni_3N-NF-2	29.9	0.0702	20.98
Ru/Ni_3N-NF-3	24.5	0.0736	18.03

Table S2. HOR performance comparison of reported HOR catalysts in 0.1 M KOH

Catalyst	i_0 (mA cm_{geo}^{-2})	$i_{0,\,m}$ (mA ug_{metal}^{-1})	Catalyst loading (ug_{PGM} cm^{-2})	Ref
$PtRu/Mo_2C$−TaC	3.78	0.29	13	[17]
P−Ru/C	-	0.43	6.06	[20]
CeO_x-Pd/C	-	0.052	13	[38]
Ru–Ir/C	-	0.62	7.8	[39]
$(Pt_{0.9}Pd_{0.1})_3Fe$	-	0.31	5	[40]
$Pd_{0.33}Ir_{0.67}$/N-C	-	0.48	10	[41]
RuNi1	-	0.28	25	[42]
Pt_3Co	2.40	0.29	~ 8	[43]
Pd_3M@Pt/C	-	0.69	5	[44]
RuRh-OM	1.91	-	-	[45]
Ir@Pd	7.18	-	20	[46]
Ru/PEI-XC	2.92	-	21.7	[21]
PtMo-CeO_x-NAs	-	0.23	10	[47]
Rh@$Pt_{0.83}$ NBs	1.97	0.21	~10.2	[48]
Ir/Mo−MoO_2	-	0.046	25	[49]
Ru/Meso C	-	0.54	25.4	[50]
Mo-Pt/NC	11.45	-	-	[51]
IrO_2-PdO/C	8.07	0.38	21	[52]
Pt/C	-□	0.25	-□	[20]
Pt/C	-	0.18	-	[40]
Pt/C	-□	0.35	-□	[49]
Ru/Ni_3N-NF	15.69	0.8	19.56	This work

Table S3. HER performance comparison of reported HER catalysts in 0.1 M KOH

Catalysts	η_{10} (mV)	iR-corrected	Ref
Pt-Ni/C	about 60	○	[56]
CP/MoS_2-$CoNi(OH)_2$	178	○	[57]
MoWN/MoWC@N-C-800	170	90%	[58]
α-$Ni(OH)_2$/Pt	124	○	[59]
CoDNG900	193	○	[60]
NiFe@Pt(111)	70	85%	[61]
W-SA	85	○	[62]
WO_x-PtNi@Pt DNWs/C	24	95%	[63]
Fe_3O_4@graphite sheets	120	-	[64]
Ni@N-C NT/NRs	134	○	[65]
CuCo-N_x@N-CCs-700	319	○	[66]
Au NPs/TiH_2/nanogrooved Ti	126	○	[67]
Ru/Ni_3N-NF	22.6	85%	This work
Pt/C	120	90%	[58]
Pt/C	79	○	[60]
Pt/C	78	○	[62]
Pt/C	72	95%	[63]
Pt/C	54	○	[65]
Pt/C	41.4	85%	This work